Arch. Metall. Mater., Vol. 61 (2016), No 4, p. 1813–1818

DOI: 10.1515/amm-2016-0293

LUO JUNTING*,**,#, XUE YAHONG*, LIU YONGKANG *, LI JIANYONG *, ZHAO SHUANGJING*

STRESS AND STRAIN ANALYSIS AND MICROSTRUCTURE OF Al/Cu CLAD COMPOSITE FABRICATED BY COLD EXTRUSION

A five-zone describing model for extrusion of aluminum/copper clad composite was established. Stress and strain were also analyzed by finite element method. The distribution rules of grain size were researched by critical shear strain theory, and zoning phenomenon of grain size was discovered. The grain size of deformed aluminum material becomes gradually finer from center to the interface. The grain size is much fine and the critical shear strain reaches the maximum value in the interface. The grain size of copper material reduces gradually from center to both the interface and exterior surface, which is caused by the higher value of critical shear strain in the interface and exterior surface. The analysis results were verified by microstructure observation and mechanical properties test, indicating that the distribution of grain size for cold extrusion forming can be interpreted by critical shear strain theory.

Keywords: aluminum/copper clad composite; cold extrusion; microstructure; critical shear strain; finite element method

1. Introduction

The use of clad material as a structural material is increasing in many industries because it has material properties that cannot be obtained from a single material [1,2]. Metal composite wire is a kind of clad composite material, which uses metal material as the core, with the outer layer coating or plating a good conductive copper or aluminum. Clad composite wire can make full use of the high strength of the core and the electrical conductivity of the coating, and expand the application scope. At present, types of composite wires are as follows: aluminum/copper clad composite, steel/copper clad composite, steel/aluminum clad composite and carbon fiber-reinforced aluminum, etc. [3-7].

The wide application of the metal composite makes the forming technology develop rapidly. At present, the preparation technologies of metal composites include cold extrusion, continuous extrusion, hydrostatic extrusion, extrusion coating, electroplating, etc. [8-11]. Products produced by these processes either have poor metallurgical bonding properties between copper and aluminum (plating aluminum wire with copper method, coated welding method, the traditional extrusion method and continuous extrusion method, etc.), or are fabricated by more complex technology which with lower productivity and higher costs (hydrostatic extrusion method).

New casting-extrusion technology aims to improve the metallurgical bonding between copper and aluminum has been presented by authors [12,13]. The technology can achieve metallurgy combination at atom levels in copper/aluminum interface, and improve the quality of Al/Cu clad composite. The double-metal composite is quite different from single material during casting-extrusion forming procedure[14,15]. Therefore, the study of the stress state and deformation characteristics of the clad composite material during extrusion process is of great significance in the controlling the products' microstructure and mechanical properties.

In the current study, aluminum/copper clad composite taken as an example, stress state and distributed law were analyzed during deformation by finite element technology. The microstructure of products was observed and the distribution rules of grain size were researched by critical shear strain theory.

2. Materials and methods

2.1. Finite element simulation

Finite element model of simplified 1/4 axial symmetry were established by DEFORM software to simulate extrusion deformation process. The finite element model is shown in Fig .1. Parameters of material properties for pure copper and aluminum are shown in Table 1. The flow stress−strain curve of material is represented by a bilinear kinematic hardening model, which is taken from the material database of DEFORM software. The relevant parameters in the process of simulation are summarized in Table 2.

* EDUCATION MINISTRY KEY LABORATORY OF ADVANCED FORGING & STAMPING TECHNOLOGY AND SCIENCE, YANSHAN UNIVERSITY, QINHUANGDAO 066004, CHINA

** STATE KEY LABORATORY OF METASTABLE MATERIALS SCIENCE AND TECHNOLOGY, YANSHAN UNIVERSITY, QINHUANGDAO 066004, CHINA

Corresponding author: luojunting@ysu.edu.cn

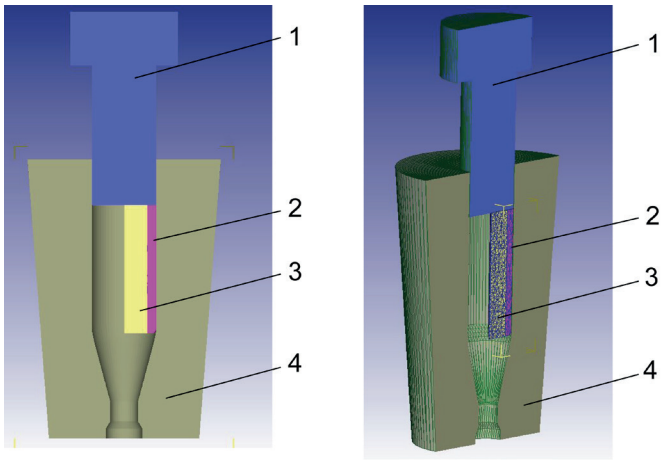

Fig. 1. FEM model of extrusion forming for aluminum/copper clad composite: 1 – Male die; 2 – Copper; 3 – Aluminum; 4 – Cavity die

2.2. Experimental process

The experiment was carried out under room temperature. Billets for the test were aluminum/copper clad composite billets, which were fabricated by low-pressure casting technology. The mixture of grease and graphite was used as lubricant. Experiments were conducted with an equipment of YA315 hydraulic press. The billet size and the deformation parameter were the same as those in finite element simulation shown in TABLE 2. Self-designed extrusion dies were used during extrusion procedure. The specific extrusion experiment can refer to related literatures [16,17].

After the extrusion, the microstructure of the samples was observed by Zeiss optical microscope (OM) and Hitachi TM3000 tabletop scanning electron microscope (SEM). The samples were cut along the radial direction in the cone-shaped deformation zone and along the axial direction near the interface. The surfaces were polished by metallographic abrasive paper and polishing machine. Because of the difference between corrosion-resistant of aluminum and copper material, different etching solutions were used to corrode copper and aluminum materials separately. Etching solution for aluminum was hydrofluoric acid and nitrate aqueous solution, while etching solution for copper was nitric acid and high-iron alcohol solution.

3. Results and discussion

3.1. Analysis of stress and strain

The five zone describing model for extrusion forming of aluminum/copper clad composite is shown in Fig. 2. The deformation region is divided into five zones, namely A, B, C, D and E. A is the area nearing the centerline in the cone-shaped deformation region. B is the area of the aluminum material in the cone deformation region. C is the area of the interface between the copper and aluminum. D is the area of the copper material in the cone-shaped deformation region, and E is the surface of the deformable body contacted with the die. A cross-section in the cone-shaped deformation region is chosen, and one point in each area of A, B, D and E are selected and they are marked 1, 2, 4 and 5, respectively. Two points are selected in C zone. One is on aluminum surface marked 3-1 and the other is on copper surface marked 3-2. When the materials are completely forced out during deformation in finite element simulation, all the value of the principal stress ($\sigma_1, \sigma_2, \sigma_3$) and the

TABLE 1

Parameters of material properties

Materials	Tensile strength /MPa	Yield strength /MPa	Elastic modulus /GPa	Elongation %	Poisson ratio
Copper	230	70	107.9	45-50	0.35
Aluminum	100	45	68	35-40	0.3

TABLE 2

Parameters of numerical simulation

Parameters	Numerical value
Extrusion temperature/°C	20
Extrusion speed/(mm·s^{-1})	10
Extrusion ratio	5.45/9
Billet length/mm	60
Outer diameter of copper tube /mm	29.8
Inner diameter of copper tube /mm	21.4
Copper volume fraction/%	25
Extrusion modular angle, 2α/(°)	30/50
Working tape/mm	10
Friction factor between billet and female die	0.25
Friction factor between billet and male die	0.2

TABLE 3

Stress and strain value of points in Fig. 2

Points	σ_1	σ_2	σ_3	τ_{max}		ε_1	ε_2	ε_3	γ_{max}
	Mpa								
1	-182	-321	-356	87		0.7710	-0.3130	-0.4710	1.2420
2	-148	-247	-370	111		1.5810	-0.7506	-0.8832	1.6338
3-1(Al)	-189	-291	-321	66		1.6930	-0.5866	-0.9328	2.6258
3-2(Cu)	-144	-295	-322	89		0.8051	-0.2655	-0.5448	1.3499
4	-219	-330	-350	65		0.4360	-0.1850	-0.2470	0.6380
5	-143	-280	-300	79		0.8353	-0.3025	-0.5267	1.3620

principal strain ($\varepsilon_1, \varepsilon_2, \varepsilon_3$) for every point are obtained, and the maximum shear stress τ_{max} and the maximum shear strain γ_{max} are calculated by the formula $\tau_{max} = (\sigma_1 - \sigma_3)/2$, $\gamma_{max} = \varepsilon_1 - \varepsilon_3$. The calculated results are shown in TABLE 3.

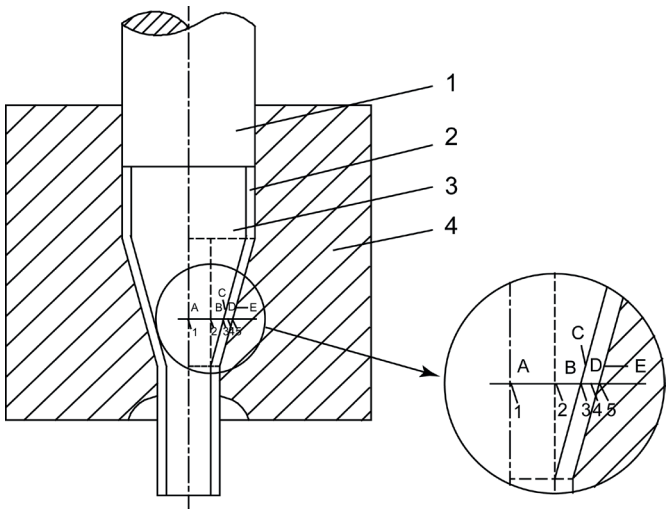

Fig. 2. Zone describing model for extrusion forming of aluminum/ copper clad composite: 1 – punch; 2 – bellit (copper); 3 – bellit (aluminum); 4 – cavity

Stress analysis in TABLE 3 shows that the stress state of all the points in the cone-shaped deformation region is the three-dimensional compressive stress, which is consistent with the characteristics of extrusion deformation. Maximum shear stress is at the point 2, which is the junction of area A and area B, and is also the junction region of the cone-shaped deformation zone and the central area. The material in the center has the trend of outflow, and cone-shaped deformation region is trapped by die angle, so that the greatest shear stress presents in this region. The maximum shear stress in point 5 is greater than that in point 4, which is mainly caused by friction between the surface of the deformable body and the interface of the squeeze tube.

Strain analysis in TABLE 3 shows that the stress-strain state of each point in the cone-shaped deformation zone is one-dimension compressive strain and two-dimensional tension strain, which is the same as strain characteristics of extrusion deformation. The largest maximum shear strain is in the aluminum surface (points 3-1) of the Cu-Al interface, and the value is greater than that in points 1 and 2, which is mainly due to the relative friction between two materials. The maximum shear strain value of copper internal surface (point 3-2) is much higher than that in the Cu center region (point 4), which indicates that the relative friction has played an important role in the improvement of shear strain. The maximum shear strain of the outer surface of the billet (point 5) is far higher than that of point 4, which also shows that the friction between the outer surface of the billet and the interface of the extrusion container play a certain role in the improvement of maximum shear strain.

During the cold extrusion deformation, the greater of the maximum shear strain value is, the finer grain will present. As to the microstructure, the grain size of the aluminum material in the deformation region refines gradually from the center to interface because the interface withstands the greatest maximum shear strain value. For the copper materials in deformation region, because the friction being subjected to its inside and outside has a greater shear strain state, the grain size becomes smaller from the center to the two surfaces.

3.2. Microstructure of original billet

The microstructure of the original billet is shown in Fig. 3. Fig. 3(a) shows that the grain shape of copper is irregular and the diameter is about 40-50 μm. Fig. 3(b) shows that the microstructure of aluminum has more evenly and equiaxed grains with a diameter of about 70-75 μm. Both two materials are large grain size, which is of the typical cast organization.

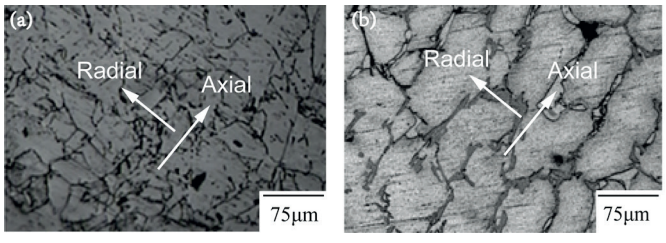

Fig. 3. OM micrograph of raw materials: (a) Microstructure of original copper billet; (b) Microstructure of original aluminum billet

3.3. Microstructure of materials in cone-shaped deformation zone

The microstructure of aluminum in cone-shaped deformation zone is shown in Fig. 4. As shown in Fig. 4(a), when the material enters into the cone-shaped deformation zone in the initial stage, aluminum grains in the interface

are beginning to be refined; while the grains in the center remain the original state. Its organization is large and uneven, and the boundaries between the refined region and the large grain region is obvious. This uneven organization is mainly due to different deformation extent between the outer layer and the central part of the metal. Large deformation in the interface leads to uneven microstructure along the radial. The thickness of interface is about 5 μm, which is obviously thinner than casting billet. As shown in Fig. 4(b), when the material reaches nearing the die outlet, the grain size of aluminum becomes smaller. The grain size in central area is also refined obviously, with an average diameter of 15−20 μm, and the grain size near the interface zone is about 10−15 μm. The interface thickness is further reduced.

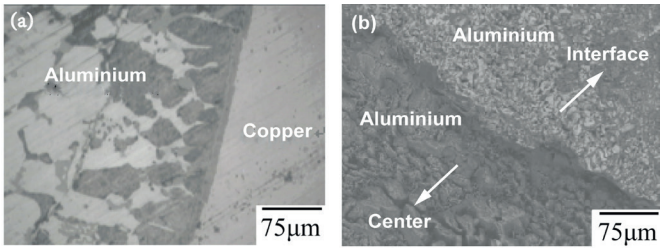

Fig. 4. OM micrograph of aluminum in cone-shaped deformation zone at the initial stage (a), SEM image of aluminum when reaches nearing the die outlet (b)

The microstructure of copper in cone-shaped deformation zone is shown in Fig. 5. Fig. 5(a) shows the microstructure of copper in the interface of aluminum/copper, and Fig. 5(b) shows the microstructure of copper on the surface of the material. Copper grain is refined obviously in the interface of aluminum/copper, and formed into an equiaxed shape, with an average diameter of 20-25 μm, which shows that recrystallization in this region plays a key role in grain refinement. Copper grain size in the center is larger, with an average diameter of 35-40 μm. Copper grain on the surface of the deformed is the smallest, with an average diameter of 10-15 μm, but the grain shape is irregular, which indicates that the shear deformation has played a major role in grain refinement.

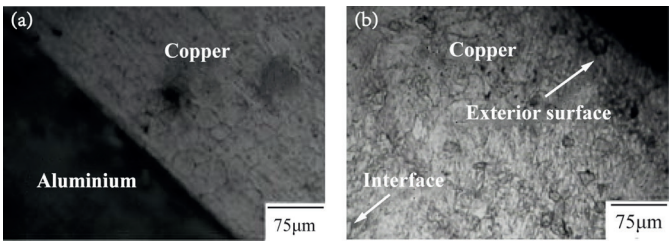

Fig. 5. OM micrograph of copper in cone-shaped deformation zone: (a) Microstructure of copper in interface; (b) Microstructure of copper in surface

3.4. Microstructure of materials after extrusion

The microstructure of aluminum after extrusion is shown in Fig. 6. Fig. 6(a) indicates the microstructure of aluminum in radial cross-section, and Fig. 6(b) indicates the microstructure of aluminum in the radial cross-section near the interface of aluminum/copper. After complete extrusion, the grains are refined and formed into uniformly distributed small grains, with an average diameter of smaller than 5 μm. In the axial section near the interface, a lot of fine and fibrous organization along the extrusion direction can be found, which is mainly caused by the shear strain at the interface during the extrusion process.

Results of microstructure observation are exactly the same as that of the simulation analysis, proving that the maximum shear strain theory can analyze grain refinement in the process of cold extrusion deformation.

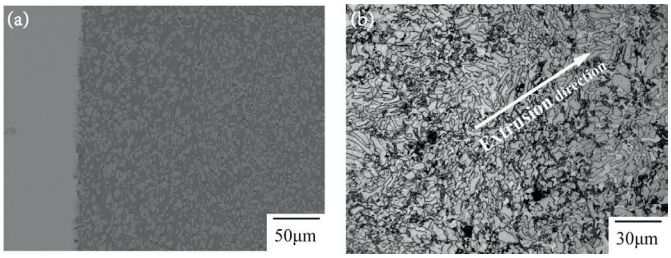

Fig. 6. SEM image of aluminum after extrusion: (a) In radial cross-section; (b) In axial cross-section near the interface

3.5. Mechanical properties

The hardness increases with the decrease of the grain for normal materials, which meets the Hall - Patch relation [18]:

$$H = H_0 + kd^{-1/2} \quad (1)$$

Where H is the hardness; H_0 is a constant; k is a coefficient; d is the average grain size.

Therefore, according to this relation, the analytical mechanics and micro structure analysis results can be validated by measuring the hardness value. The hardness and elastic modulus of products after extrusion were measured with nanoindentation testing system. Six points were selected along the circumferential direction of same radius, and taken the average value. The maximum force was 2000 N. Both the holding pressure time and the uniform unloading time were 10 s. The radius coordinates of measuring points and the measuring results are shown in Fig. 7 and Fig. 8, respectively. Points 1, 2 and 3 are for coated copper layer on the products surface. Point 1 is the higher hardness value because it is close to the outer surface and the hardness value of point 2 decreases slightly, but the hardness value of point 3 is increased again as it approaches the interface region. The hardness is the maximum value for points 4, 5and 6, in the interface region, which is mainly due to the formation of $CuAl_3$ alloy with fine grains [17]. The hardness values for points 8, 9 and 10 gradually reduce from the interface to the center for pure aluminum. All of the above tested results are completely consistent with the results of mechanics and microstructure analysis. The variation trend of elastic modulus is opposite to hardness.

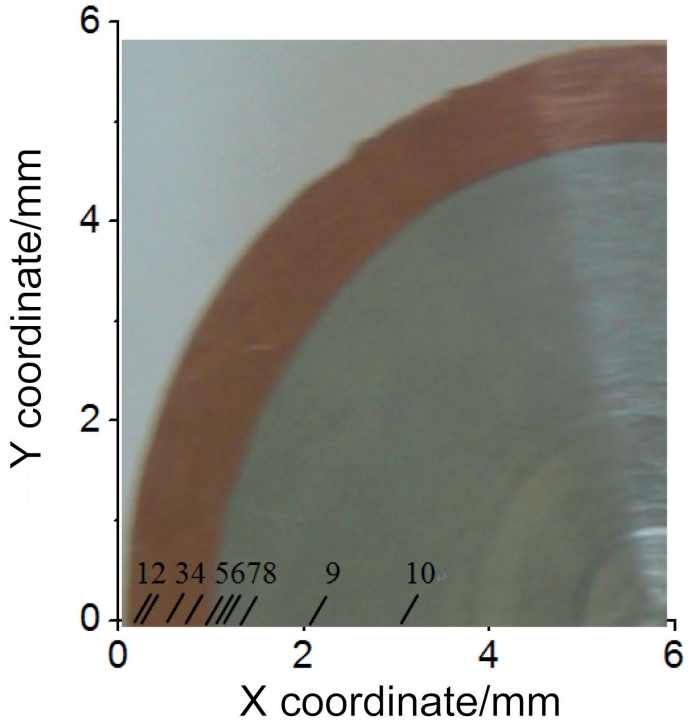

Fig. 7. Radius coordinate diagram of measuring points

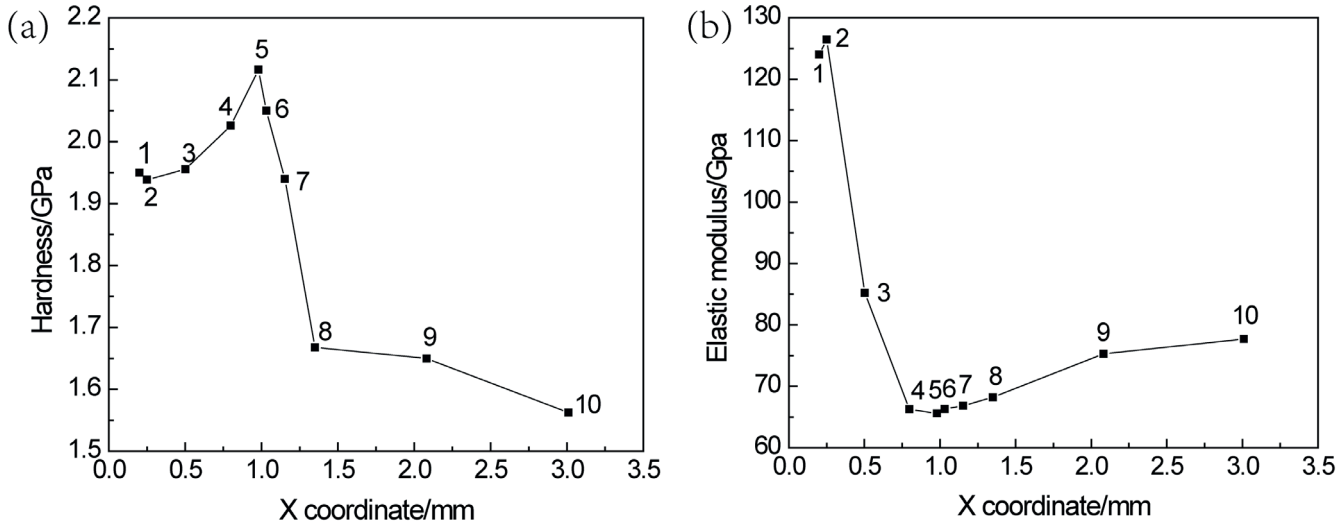

Fig. 8. The test results of mechanical properties: (a) Hardness; (b) Elastic modulus

4. Conclusions

The grain size distribution in extrusion deformation of Bi-metal composite material is different from that in a single metal extrusion deformation. The grain size presents obvious geographical phenomena for cold extrusion of Bi-metal composite material. Grain size close to the interface of aluminum/copper is much smaller than that of far from the interface. The stress-strain state in the extrusion deformation process can be analyzed, and the microstructure and mechanical property distribution of the material can be explained and forecasted by finite element simulation technology.

Acknowledgments

This research was funded by Natural Science Foundation of Hebei Province, China(E2012203086). The authors are grateful to all their support.

REFERENCES

[1] J.S. Lee, H.T. Son, I.H. Oh, C.S. Kang, C.H. Yun, S.C. Lim, H.C. Kwon, J. Mater. Process. Tech. 187-188 (12), 653-656 (2007).

[2] I.S. Son, S.P. Lee, J.K. Lee, W.C. Kim, J.S. Moon, T. Nonferr. Metal. Soc. **24**, 75-80 (2014).
[3] A. Khosravifard, R. Ebrahimi, Mater. Design. **31** (1), 493-499 (2010).
[4] D.C. Ko, S.K. Lee, B.M. Kim, H.H. Jo, H. Jo, J. Mater. Process. Tech. **186** (1–3). 22-26 (2007).
[5] X. Guo, H. Wang, Z. Liu, L. Wang, F. Ma, J. Tao, Int. J. Adv. Manuf. Techno. **82** (1), 1-6 (2015).
[6] X.H. Chen, X. Tang, Z.D. Wang, X.D. Hui, M. Li, Y.W. Wang, Int. J. Min. Met. Mater. **22** (2), 190-196 (2015).
[7] E.W. Jeong, K.N. Hui, D.H. Bae, D.S. Bae, Y.R. Cho, Met. Mater.- Int. **20** (3), 499-502 (2014).
[8] Z. Chen, K. Ikeda, T. Murakami, T. Takeda, J.X. Xie, J. Mater. Process. Tech. **137**, 10-16 (2003).
[9] J.X. Xie, C.J. Wu, X.F. Liu, X.H. Liu, Mater. Sci. Forum. 539-**543**, 956-961 (2007).
[10] H.J. Park, K.H. Na, N.S. Cho, Y.S. Lee, S.W. Kim, J. Mater. Process. Tech. **67**(1), 24-28 (1997).
[11] C.G. Kang, Y.J. Jung, H.C. Kwon, J. Mater. Process. Tech. **124**, 49-56 (2002).
[12] J.T. Luo, Y. Xu, S.J. Zhao, Appl. Mech. Mater. **16**-19, 441-444 (2009).
[13] C.G. Kang, H.C. Kwon, Int. J. Mech. Sci. **44**(2), 247-267 (2002).
[14] E. Hug, N. Bellido, Mater. Sci. Eng. A. **528**(22), 7103-7106 (2011).
[15] V.Y. Mehr, M.R. Toroghinejad, A. Rezaeian, Mater. Design. **53**(1), 174-181 (2014).
[16] J.T. Luo, S.J. Zhao, C.X. Zhang, J. Cent. South Univ. T. **19** (4), 882-886 (2012).
[17] J.T. Luo, S.J. Zhao, J. Cent. South Univ. T. **18** (4), 1013-1017 (2011).
[18] J.H. Kim, M. Nakamichi, J. Nucl. Mater. **453** (1–3), 22-26 (2014).